



# Karbala International Journal of Modern Science

Manuscript 3397

## Evaluating the New Nd: YAG Laser Method in Phytosynthesizing Silver Nanoparticles and Assessing Their Medical Applications.

Arshad Mahdi Hamad

Qanat Mahmood Atiya

Follow this and additional works at: <https://kijoms.uokerbala.edu.iq/home>



Part of the [Biology Commons](#), [Chemistry Commons](#), [Computer Sciences Commons](#), and the [Physics Commons](#)



---

# Evaluating the New Nd: YAG Laser Method in Phytosynthesizing Silver Nanoparticles and Assessing Their Medical Applications.

## Abstract

Silver nanoparticles (AgNPs) were synthesized via an innovative green synthesis method using amygdalin (Am) as a reducing agent and the Nd: YAG laser as a catalyst. We studied the properties of the nanoparticles using X-ray diffraction (XRD), field emission scanning electron microscopy (FESEM), energy dispersive X-ray spectroscopy (EDX), atomic force microscopy (AFM), ultraviolet-visible spectroscopy (UV), and Fourier transform infrared spectroscopy (FTIR) techniques. All the results of the examination demonstrate excellent structural and optical properties. In addition, the molecular docking of the complex composed of amygdalin and AgNPs was tested on three proteins concerned with the virulence of *Pseudomonas aeruginosa* and their resistance to antibiotics. These proteins, 4QU3, 7MQK, and 2UWJ had -6.82, -6.64, and -6.41 binding affinity (kcal/mol), respectively. The antimicrobial activity was tested on multi-drug-resistant (MDR) *P. aeruginosa* isolates from wounds and burns, confirming their potential as effective antibacterial agents, with the inhibition rate reaching (20.73 mm) for wound isolations at a concentration of (5 mM) for Am-AgNPs. A cytotoxicity test (MTT) was tested for (24 h) on human dermal fibroblasts (HDFn) and human melanoma cells (A375). Compared to the normal cell line, the outcomes against the cancer line were exceptional. The objective of this research is to rapidly produce AgNPs in an environmentally favorable manner. The therapeutic efficacy of Am-AgNPs against MDR *P. aeruginosa* isolated from wounds and burns, as well as the synthetic nanomaterial's efficacy against the skin cancer line, creates new opportunities for the treatment of intractable diseases caused by bacteria that are resistant to antibiotics, in addition to cancer.

## Keywords

Am-AgNPs; Amygdalin; Nd: YAG; *P. aeruginosa*; HDFn; A375

## Creative Commons License



This work is licensed under a [Creative Commons Attribution-Noncommercial-No Derivative Works 4.0 License](https://creativecommons.org/licenses/by-nc-nd/4.0/).

## RESEARCH PAPER

# Evaluating the New Nd: YAG Laser Method in Phytosynthesizing Silver Nanoparticles and Assessing Their Medical Applications

Arshad M. Hamad<sup>\*</sup>, Qanat M. Atiya

Department of Biology, College of Science, University of Tikrit, Tikrit, Iraq

### Abstract

Silver nanoparticles (AgNPs) were synthesized via an innovative green synthesis method using amygdalin (Am) as a reducing agent and the Nd: YAG laser as a catalyst. We studied the properties of the nanoparticles using X-ray diffraction (XRD), field emission scanning electron microscopy (FESEM), energy dispersive X-ray spectroscopy (EDX), atomic force microscopy (AFM), ultraviolet-visible spectroscopy (UV), and Fourier transform infrared spectroscopy (FTIR) techniques. All the results of the examination demonstrate excellent structural and optical properties. In addition, the molecular docking of the complex composed of amygdalin and AgNPs was tested on three proteins concerned with the virulence of *Pseudomonas aeruginosa* and their resistance to antibiotics. These proteins, 4QU3, 7MQK, and 2UWJ had  $-6.82$ ,  $-6.64$ , and  $-6.41$  binding affinity (kcal/mol), respectively. The antimicrobial activity was tested on multi-drug-resistant (MDR) *P. aeruginosa* isolates from wounds and burns, confirming their potential as effective antibacterial agents, with the inhibition rate reaching (20.73 mm) for wound isolations at a concentration of (5 mM) for Am-AgNPs. A cytotoxicity test (MTT) was tested for (24 h) on human dermal fibroblasts (HDFn) and human melanoma cells (A375). Compared to the normal cell line, the outcomes against the cancer line were exceptional. The objective of this research is to rapidly produce AgNPs in an environmentally favorable manner. The therapeutic efficacy of Am-AgNPs against MDR *P. aeruginosa* isolated from wounds and burns, as well as the synthetic nanomaterial's efficacy against the skin cancer line, creates new opportunities for the treatment of intractable diseases caused by bacteria that are resistant to antibiotics, in addition to cancer.

**Keywords:** Am-AgNPs, Amygdalin, Nd: YAG, *P. aeruginosa*, HDFn, A375

## 1. Introduction

The skin serves as an ideal medium for the proliferation of pathogenic bacteria which can worsen the condition of wounds and burns due to the inflammatory aspect caused by the settlement and invasion of these bacteria [1]. Wounds, whether post-surgical or due to trauma or accident [2], are susceptible to contamination by pathogenic bacteria, particularly those that are multi-drug-resistant (MDR) pathogens. This contamination will result in increased infection risk and impaired healing due to the exacerbation of antibiotic failure, which

has exacerbated the mortality rate [3]. Contaminated burn injuries are the dominant cause of death, especially burns contaminated with MDR pathogens such as *Pseudomonas aeruginosa*, methicillin-resistant *Staphylococcus aureus* (MRSA). The presence of these microorganisms in burn injuries is a critical marker of failed healing [4]. It is common to isolate *P. aeruginosa*, a Gram-negative bacterium, from various sites in the human body, including wounds, burns, urinary tract infections, middle ear infections, and post-surgical infections [5]. It is highly susceptible to genetic changes that lead to antibiotic resistance, especially in immunocompromised individuals.

Received 22 November 2024; revised 14 January 2025; accepted 18 January 2025.  
Available online 12 February 2025

\* Corresponding author.  
E-mail address: [Arshad.m.hamad@tu.edu.iq](mailto:Arshad.m.hamad@tu.edu.iq) (A.M. Hamad).

<https://doi.org/10.33640/2405-609X.3397>

2405-609X/© 2025 University of Kerbala. This is an open access article under the CC-BY-NC-ND license (<http://creativecommons.org/licenses/by-nc-nd/4.0/>).

Given the acquired and inherent nature, this bacterium resists antibiotics. Thus, its eradication is increasingly challenging [6]. As a result, there is an increasing demand to provide and develop new alternatives to combat pathogens. The occurrence of resistance has been exacerbated by the imprudent administration of antibiotics, particularly in developing countries, as a result of their dispensation without a prescription, resulting in the emergence of MDR strains more commonly [7,8]. In this context, numerous studies in the field of nanotechnology have documented the antibacterial activity of many metallic nanoparticles, which are increasingly gaining attention in medicine as new alternatives, with particular efficacy against MDR strains [9,10]. Nanoparticles of a given metal exhibit unique properties compared to their large-sized counterparts [11]. Nanomaterials, a unique class of materials with dimensions ranging from (1 to 100 nm) possess unique and distinctive properties and find extensive applications in various fields. These particles interact with vital organic components on the surface of microorganism cells, resulting in structural degradation [12]. Silver nanoparticles (AgNPs) are metallic silver particles with a small size ranging from one to one hundred nanometers. As a result, they have a large surface area relative to their small size, which increases their ability to interact with other elements [13]. Ointments and dressings for burns, containing silver nitrate or silver sulfadiazine, have utilized silver's antibacterial properties [14,15]. Researchers studied the antibacterial ability of AgNPs when nanotechnology emerged. Simultaneously, it plays a crucial role in the food packaging, electronics, and agriculture industries. Due to the unique properties of AgNPs, it is the most common and widely used nanoparticle. AgNPs exhibit a variety of biological activities, including antibacterial, antiviral, anti-fungal, and anticancer effects [16]. Due to the variety of readily available plants and their simple and safe application, plant synthesis of AgNPs is a widely used strategy. The green synthesis of nanoparticles has effectively used many plant parts, including leaves, extracts, fruits, and flowers. Plant extracts contain a collection of bioactive compounds, such as vitamins, enzymes, terpenoids, tannins, sugars, phenolics, and flavonoids. The presence of these functional biomolecules in plant extracts enhances the stability and efficacy of the synthesis of bioactive AgNPs using plants [17]. The green synthesis of Am-AgNPs in this research utilized amygdalin, a cyanogenic compound also known as bitter apricot, laetrile, or almond. It belongs to the aromatic cyanogenic glycoside group. Its molecular formula is  $C_{20}H_{27}NO_{11}$  [18], and the seeds of apple, cranberry,

peach, and plum plants belonging to the Rosaceae family widely distribute it, with the seeds of apricot kernels being especially rich in it. Recent studies have noted its effectiveness in treating tumors [19]. Many studies have proven its anti-asthma and anti-ulcer effects. Moreover, its pharmacological effects encompass inhibition of interstitial renal fibrosis, prevention of pulmonary fibrosis, resistance to hyperoxia-induced immunosuppression, lung injury, anti-tumor, anti-inflammatory, immunoregulation, and antiulcer properties [20,21]. Amygdalin's property to destroy cancer cells by blocking their sources of nutrients contributes to its effectiveness in treating cancer. Many Western countries have found it to reduce the incidence of prostate, colon, and rectal cancers, and are currently incorporating it into their treatment protocols for cancer patients [18]. The Nd: YAG laser provides controlled and precise energy pulses that are used in the physical method of creating nanoparticles, known as laser ablation, where laser pulses are directed to the surface of any metal immersed in a liquid to start the process of surface ablation and produce nanoparticles [22]. The Nd: YAG laser represents a strong catalyst in oxidation and reduction processes, so it was chosen to stimulate the reaction and produce AgNPs [23]. This study aims to evaluate the green synthesis of AgNPs using amygdalin extract and Nd: YAG laser as a catalyst and then study its biological activities, including antimicrobial and cytotoxic activities. Additionally, it will study the molecular docking and simulation of specific proteins.

### 1.1. Ethics approval

This study was conducted in compliance with ethical principles. The study protocol, subject information, and consent form were approved by the local ethics committee according to administrative order No. THU00004 dated 10/17/2024.

## 2. Materials and methods

### 2.1. Novel green synthesis

In this method, we did not use heating or a chemical catalyst, and the material was not left at room temperature for (7 h) or even (24 h), but rather an Nd: YAG laser was used, specifically with a wavelength of (355 nm), and a repetition rate (10 Hz), and an energy of (100 mJ). Thus, the pulses of this laser were directed to this mixture of  $AgNO_3$  at a concentration of (5 mM) in a volume of (50 mL), and (60  $\mu$ L) of amygdalin at a concentration of (2 %) was added to it. The laser pulse was distributed

throughout the solution by rotating a rotor at a rate of (30 rpm). After (600 pulses) of the Nd: YAG laser, a color change occurred, and thus it was the first sign of the formation of Am-AgNPs. The innovative laser method for green synthesis of Am-AgNPs has the advantage of requiring no time for the synthesis process, with an estimated duration of 1 min, whereas other methods require a duration ranging from several hours to a whole day. The use of Nd: YAG laser is environmentally friendly and does not lead to the formation of toxic fumes, such as in the hot or chemical method or produce harmful waste. In this case, our innovative method does not require time and is environmentally friendly.

## 2.2. Am-AgNPs characteristics

The structural and optical analyses of the prepared Am-AgNPs were performed using XRD, and the crystal volume was calculated according to the Debye-Scherrer equation (1) [24].

$$D = K\lambda / \beta \cos(\theta). \quad (1)$$

D is the crystallite size (in nanometers), K is the shape factor (typically around 0.9),  $\lambda$  is the wavelength of the X-rays used (in nanometers),  $\beta$  is the full width at half maximum (FWHM) of the diffraction peak (in radians),  $\theta$  is the Bragg angle of the peak (in radians). Techniques such as FESEM, EDX, AFM, UV-Visible spectroscopy, and FTIR are utilized. These techniques provide accurate information about the crystal structure, surface composition, elemental composition, surface topography, and optical and vibrational properties of the samples.

## 2.3. In silico molecular docking study

The molecular docking exploration was conducted using the AutoDock Vina tool [25]. The crystallography structures of three proteins (PDB ID: 4QU3, 7MQK, and 2UWJ) were obtained from the Protein Data Bank (PDB) with resolutions of (1.40, 1.60, and 2.00 Å) respectively, for docking at the Research Collaboratory for Structural Bioinformatics <http://www.RCSB.org>. The ChemSketch was used for drawing the 3D (MOL format) chemical structure of artificial ligands <http://www.cambridgesoft.com/software/overview.aspx>. The PDB File (PDB format) target structure has been prepared. The co-crystallized ligands were identified and removed before processing. Water molecules were detached; both polar and nonpolar hydrogens were added. To analyze interactions, we utilized the BIOVIA Discovery Studio Visualizer (DSV) Client 2021 <https://discover.3ds.com/>

[discovery-studio-visualizer-download](#) for creating two-dimensional (2D) and three-dimensional (3D) interactions.

## 2.4. Antibacterial screening of Am-AgNPs

The isolates of MDR *P. aeruginosa* were obtained from Tikrit Teaching Hospital after they were isolated and diagnosed according to standard methods from patients with wound and burn infections admitted to the hospital [12]. The inhibitory activity was assessed using the well diffusion agar method, where Mueller Hinton plates were prepared. The density of the bacterial suspension was calibrated to 0.5 McFarland. The bacteria were cultured on the surface of the plate. Six wells, each with a diameter of (5 mm), were then created on the surface of the agar plates using a sterile cork borer, one of which was for the control, then the Am-AgNPs solution prepared at concentrations of (5, 4, 3, 2, and 1 mM) was added, where it was added in a volume of 50  $\mu$ L for each well using a micropipette. The plates were incubated at (37 °C) for (24 h), and the inhibition zone was measured in millimeters using a standard ruler [12].

## 2.5. Cytotoxicity effect of Am-AgNPs

The cytotoxicity of Am-AgNPs was detected by MTT [3-(4-dimethylthiazol-2-yl)-2, 5-diphenyltetrazolium bromide] assay, which was performed on human dermal fibroblasts (HDFn) and human melanoma cells (A375). Cells were cultured in DMEM with 10 % FBS and 1 % penicillin-streptomycin at 37 °C with 5 % CO<sub>2</sub>, and 95 % humidity. Cells ( $1 \times 10^4$ ) were seeded in 96-well plates, incubated for (24 h) and treated with Am-AgNPs at concentrations ranging from (3.12 to 400  $\mu$ g/ml) for an additional (24 h). After treatment, MTT solution (0.5 mg/mL) was added, and plates were incubated for (3-4 h). Formazan crystals were dissolved in DMSO, and absorbance was measured at (570 nm). Cell viability was calculated relation to controls [18]. This methodology is adapted from ISO 10993-5 for in vitro cytotoxicity testing.

# 3. Results & discussion

## 3.1. Color change

The color change is the first sign of the formation of Am-AgNPs, as mentioned in Ref. [26]. The color changes in the mixture of (5 mM) AgNO<sub>3</sub> with 2 % amygdalin were monitored in a glass beaker containing the mixture under the pulse generator arm

of the Nd: YAG laser device. The color transition from semitransparent white to dark brown occurred approximately 1 min after the application of 600 laser pulses when the Nd: YAG laser was employed, as illustrated in Fig. 1.

### 3.2. UV analysis

UV spectroscopy is one of the most widely used methods for identifying various chemicals, including organic compounds, transition metal ions, and biological molecules [27]. Fig. 2, which depicts the clear contrast in the peaks of the curves used to evaluate the absorbance of amygdalin extract and (5 mM)  $\text{AgNO}_3$  solution shows UV spectroscopy of amygdalin extract produced a single absorption peak at (270 nm). In contrast, the silver nitrate solution showed an absorption peak at (249 nm), while the absorption peak of Am-AgNPs prepared by the green synthesis method was (420 nm). This peak indicates that it matches the optimal absorbance value for AgNPs [27].

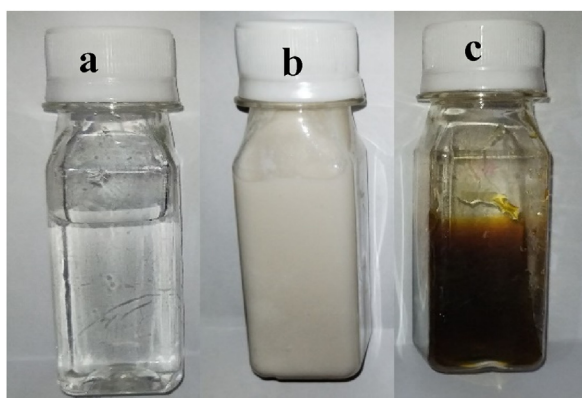


Fig. 1. Color change (a)  $\text{AgNO}_3$ , (b) Amygdalin, (c) Am-AgNPs.

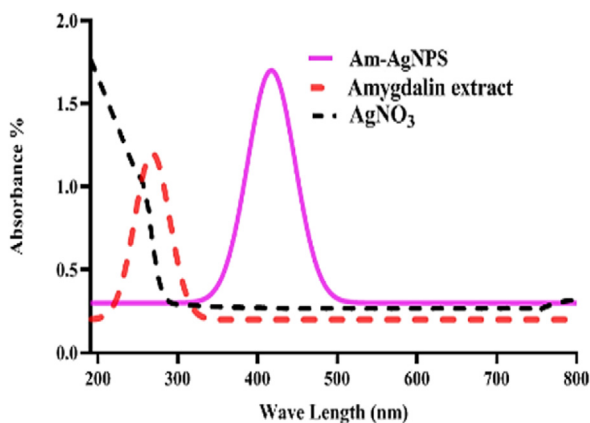


Fig. 2. UV–Vis absorption spectra of Amygdalin,  $\text{AgNO}_3$ , and Am-AgNPs.

Moreover, the absorption intensity demonstrates good homogeneity of the distribution of nanoparticles, and the presence of a larger quantity of nanoparticles. Hence, such homogeneity is owing to the quality of the interaction between the materials used during preparation [28]. The final concentration was prepared at (5 mM) and the prepared solution was examined using an Atomic Absorption Spectrometer revealing a concentration of approximately ( $400 \mu\text{g/mL}$ ), then it was titrated to ( $400 \mu\text{g/mL}$ ) by adding deionized water for use in the cytotoxicity assay.

### 3.3. XRD analysis

Fig. 3 illustrates the XRD pattern peaks obtained for the Am-AgNPs. They were prepared by the innovative green method, Am-AgNPs correspond to ( $\text{Ag}_2\text{O}$  [00-041-1104]), which makes them match with seven peaks (See Table 1).

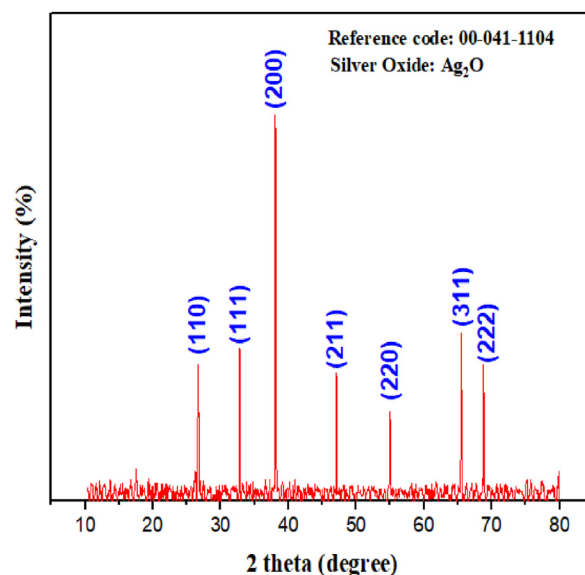


Fig. 3. XRD patterns of Am-AgNPs prepared by innovative green synthesis method. \*Special description of the title. (dispensable).

Table 1. XRD results of Am-AgNPs prepared by innovative green synthesis method.

Am-AgNPs prepared by innovative green synthesis				
2 $\theta$ (deg)	hkl	$\beta$ (deg)	d [Å]	D (nm)
26.943	110	0.18	3.34200	46.2
32.888	111	0.17	2.72900	51.33
38.014	200	0.13	2.36200	69.3
47.17	211	0.17	1.92910	53.30
55.15	220	0.2	1.67090	46.2
65.48	311	0.29	1.42500	32.23
68.89	222	0.24	1.36420	40.76
Crystal size average = 48.47 nm				

### 3.4. FESEM analysis

It is an important device for analyzing the size and shape of nanoparticles. This microscope uses a beam of electrons instead of light to form images. To display Am-AgNPs, they are placed on a special holder, usually a small copper disk (1 mm diameter) coated with a thin layer of carbon [29]. We studied the surface topology of the Am-AgNPs, already synthesized by the innovative green method, using scanning electron microscopy. The micrographs presented in Fig. 4 illustrate that the synthesized Am-AgNPs have spherical and cubic shapes. The average size of Am-AgNPs is approximately (45 nm). Based on the measurements, the standard deviation of the nanoparticles was calculated as (21.38) nm. Nanoscale dimensions of the particles prepared by the innovative green synthesis method are depicted in Fig. 5.

### 3.5. EDX analysis

The EDX spectrum of Am-AgNPs, which were prepared using the innovative green synthesis method, typically exhibited a high peak for silver at approximately 3 keV, confirming the presence of silver in the sample. This peak is a result of the characteristic X-ray emission of silver atoms when

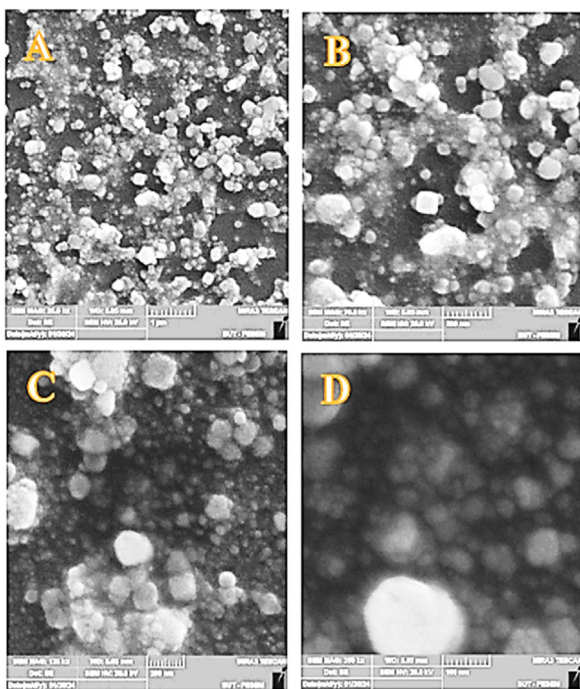


Fig. 4. SEM micrograph of Am-AgNPs prepared by innovative green synthesis method at different magnifications and scale bars (a) 1  $\mu\text{m}$  (1000x), (b) 500 nm (2000x), (c) 200 nm (6000x), (d) 100 nm (10000x).

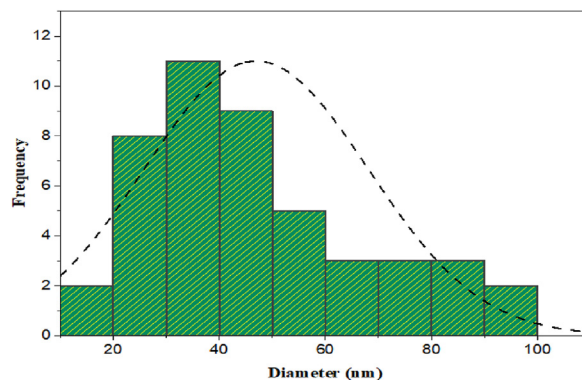


Fig. 5. Nanoscale size distribution diagram of Am-AgNPs prepared by the innovative green method.

excited by the electron beam in the EDX device. The relative abundance of silver in the sample is 70%, indicating that silver is the dominant element, constituting 70 % of the detected elements. Conversely, oxygen was 30 % at (0.4 keV), indicating that the examined compound is silver oxide, which is consistent with the XRD results, as shown in Fig. 6.

### 3.6. AFM analysis

The results of AFM examinations detected the topography of Am-AgNPs. This analysis was conducted for Am-AgNPs prepared by the innovative green manufacturing method as shown in Fig. 7 a, through a 2D image, with a cross-sectional area of (1200 nm) for the X-axis and (1200 nm) for the Y-axis. By matching with the color scale on the side of the shape, the surface size average (10-20) nm was the most frequent. As for Fig. 7 b, through a 3D image, with a cross-sectional area of (1000 nm) for the X-axis and (1000 nm) for the Y-axis. By matching with the color scale on the side of the shape, the surface size average (10-20) nm was the most

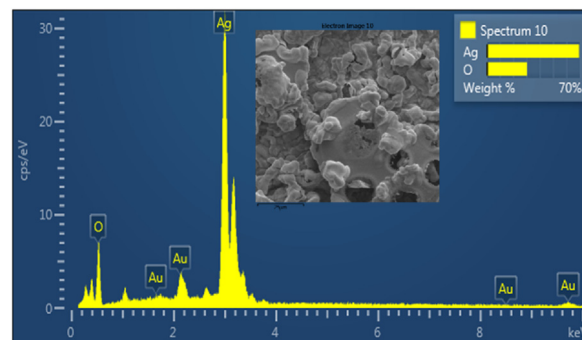


Fig. 6. EDX analysis of Am-AgNPs prepared by the innovative green synthesis method.

frequent. As for Fig. 7 c. In height histograms, it can be observed that the vast majority had dimensions less than (100 nm).

Based on the aforementioned, it is evident that the laser utilized in the innovative preparation process plays a critical and significant role in the reduction

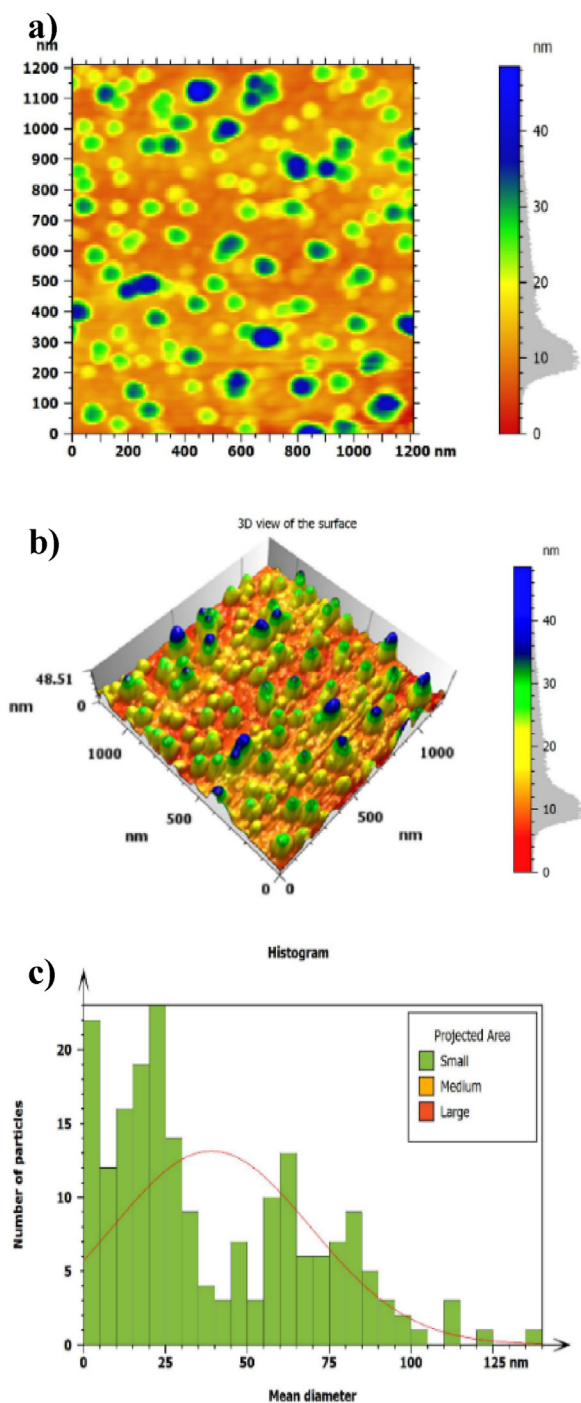


Fig. 7. AFM analysis of Am-AgNPs prepared by the innovative green synthesis method (a) 2D image, (b) 3D image, (c) Height histograms.

of nanoparticle sizes, which in turn enhances their efficacy in applications.

### 3.7. FTIR analysis

Fig. 8 displays the FTIR results as follows: The FT-IR spectrum of amygdalin (Am) extracted from apricot seeds showed absorption bands at frequency  $(3441) \text{ cm}^{-1}$  due to the stretching of the hydroxyl groups (OH) bonds. Hydroxyl bonds are present in the glucose groups attached to amygdalin, which explains the presence of these broad at distinctive peaks. An absorption band at frequency  $(1635) \text{ cm}^{-1}$  is the stretching of the C=C bond; this peak often refers to (C=C) in the molecule as it could be part of the structure of the organic compound. An absorption band at a frequency of  $1394 \text{ cm}^{-1}$  refers to the bending vibrations of the methylene group (-CH<sub>2</sub>) or other similar groups, such as C-H bending. Absorption bands at frequency  $(543) \text{ cm}^{-1}$  are due to the stretching of the (-CN) groups [30]. The FT-IR spectrum of silver nitrate (AgNO<sub>3</sub>) showed absorption bands at  $(2351) \text{ cm}^{-1}$  and  $(2061) \text{ cm}^{-1}$ . These peaks are typically the result of impurities or surface absorption that is unrelated to the parent compound and may indicate the absorption of gases, such as carbon dioxide (CO<sub>2</sub>), from the atmosphere. The range  $(1759) \text{ cm}^{-1}$  indicates the secondary decomposition of silver nitrate leading to the appearance of (NO<sub>2</sub>) groups. The range  $(1444) \text{ cm}^{-1}$  indicates the vibrations of the nitrate group (NO<sub>3</sub><sup>-</sup>), and  $(819) \text{ cm}^{-1}$  and  $(736) \text{ cm}^{-1}$ . Altogether, they represent the bending vibrations of the nitrate group (NO<sub>3</sub><sup>-</sup>), which are characteristic features of compounds containing nitrates. The range  $(412) \text{ cm}^{-1}$  indicates the vibrations of the bond between the oxygen

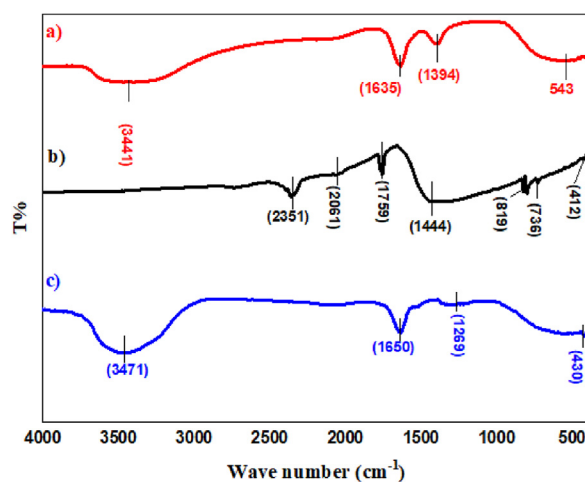


Fig. 8. FTIR analysis (a) 2 % Amygdalin extract, (b) AgNO<sub>3</sub>, and (c) Am-AgNPs prepared by the innovative green synthesis method.

element and silver [31]. When examining (FT-IR) of Am-AgNPs prepared by the innovative green synthesis method, a range of a percentage (3471)  $\text{cm}^{-1}$  was observed, which indicates the presence of a hydroxyl group (O-H) as a result of the presence of water or surface moisture, as well as the range (1650)  $\text{cm}^{-1}$ . This range signifies the existence of the (C=O) group, a component of amygdalin, and suggests a potential interaction between this group and silver during the synthesis process. This peak indicates a possible interaction between silver and organic molecules. The presence of organic bonds from compounds such as ethers or amines affixed to the Am-AgNPs was indicated by a band at (1269)  $\text{cm}^{-1}$ . This peak is associated with (C-O) vibrations, which support the notion that the nanoparticles interact with the chemical components of amygdalin. The band at (430)  $\text{cm}^{-1}$  was shown; these peaks indicate (Ag-O) vibrations [32], which reflect the presence of bonds between silver and oxygen. The spectrum indicates that the heat-free green manufacturing method has the capability of preparing Am-AgNPs.

### 3.8. Molecular docking

In this study, 7MQK, 4QU3, and 2UWJ were chosen as target proteins because 7MQK acts as (AAC (3)-IIIa), which is responsible for antibiotic resistance in *P. aeruginosa*, especially aminoglycoside antibiotics, such as gentamicin. This enzyme helps add an acetyl group to these antibiotics, thus neutralizing their effect [33]. As for the protein 4QU3, which acts as GES-2 ertapenem acyl-enzyme complex, this protein neutralizes the action of beta-lactam antibiotics by breaking the beta-lactam ring. The action of this protein is concentrated in the carbapenem antibiotic group, especially ertapenem [34]. As for the protein 2UWJ, which acts as the structure of the heterotrimeric complex in *P. aeruginosa*, it is integral to the regulation of type III secretion (T3SS) needle formation. This system, which is common among Gram negative pathogens, functions as a molecular syringe, injecting bacterial effector proteins directly into the host cell to disrupt its immune response and cellular functions. This system enhances bacterial virulence and survival within host tissues [35]. Accordingly, the choice of these proteins as targets came because they play a fundamental role in MDR strains. Therefore, neutralizing the action of these proteins represents a critical goal for eradicating these bacteria (See Table 2).

As shown in Fig. 9, the biologically active compound amygdalin-AgNPs interacts with the 4QU3 protein by forming 2 carbon-hydrogen bonds with

Table 2. The binding affinity of prepared ligands with selected proteins.

Complex	Binding Affinity (Kcal/mol)
4QU3-amygdalin-AgNP	-6.82
7MQK-amygdalin-AgNP	-6.64
2UWJ-amygdalin-AgNP	-6.41

the amino acid SER64, and a carbon-hydrogen bond with the amino acid THR232, in the active site of the protein. In addition, there are 3 conventional hydrogen bonds with the amino acid ASN127 and 3 conventional hydrogen bonds with GLU161, ARG238, and SER125 amino acids, in the active site

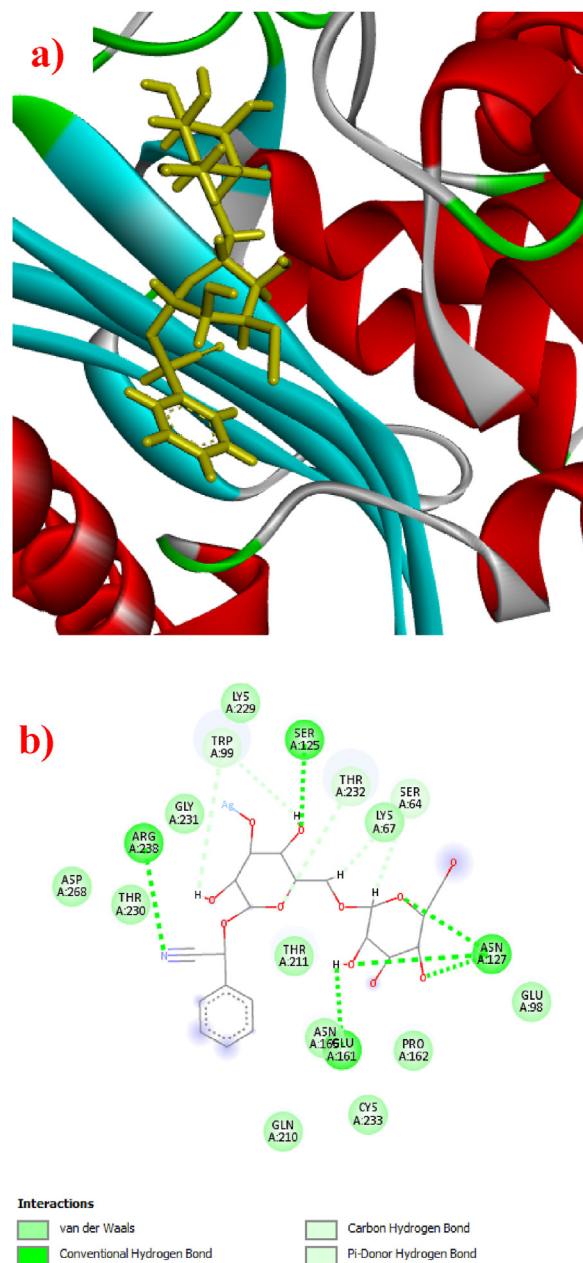


Fig. 9. The molecular docking of Amygdalin-Ag NP with 4QU3 as a target protein of *P. aeruginosa* (a) 3D, (b) 2D.

of the protein. The binding interactions suggest that the amygdalin-silver complex has the ability to modulate the function of GES-2, potentially inhibiting its carbapenem-degrading enzyme activity.

As shown in Fig. 10, the biologically active compound amygdalin-AgNPs interacts with the 7MQK protein by forming a carbon-hydrogen bond with GLU123 amino acid in its active site. Additionally, the protein's active site contains two conventional hydrogen bonds with TYR64 and GLU123 amino acids, a metal acceptor with GLU1102 amino acid, Pi-Sigma with PRO215 amino acid, and Pi-Pi stacked with PHE221 amino acid. The amygdalin-Ag complex's ability to bind to the 7MQK protein

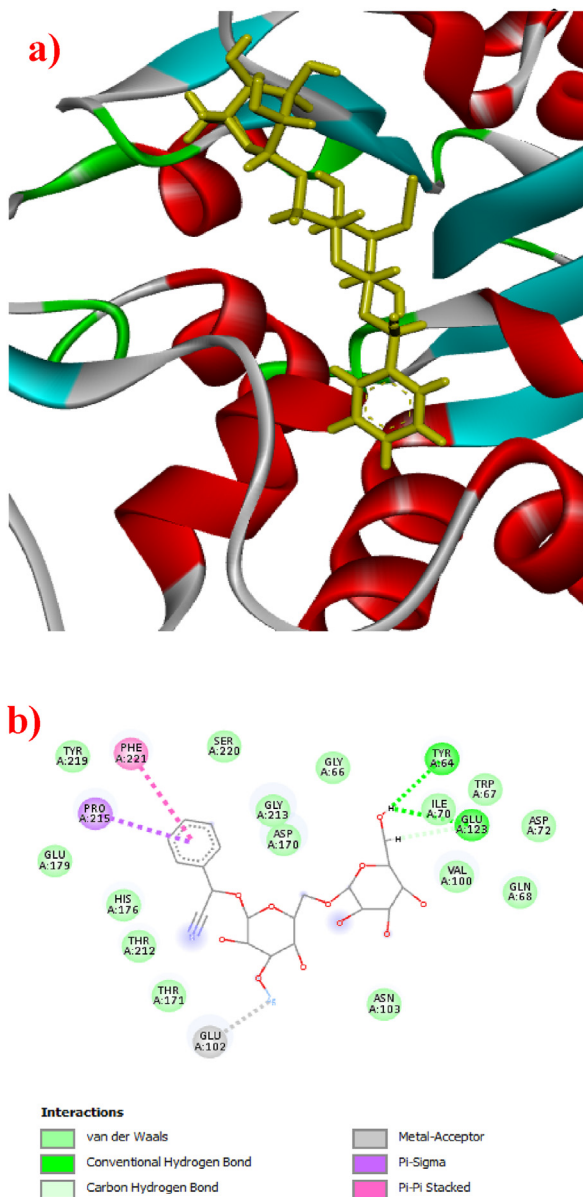


Fig. 10. The molecular docking of Amygdalin-Ag NP with 7MQK as a target protein of *P. aeruginosa* (a) 3D, (b) 2D.

may inhibit the protein's function, thereby disrupting its role in antibiotic resistance. Specifically, the Ag ion may possess additional antimicrobial properties, which could enhance the overall effectiveness of the complex.

As shown in Fig. 11, the biologically active compound amygdalin-AgNPs interacts with the 2UWJ protein by forming 5 carbon-hydrogen bonds with SER2, GLY1, SER13, GLY1, and GLU69 amino acids, and 2 carbon-hydrogen bonds with GLU9 and GLU69 amino acids, a Pi-Anion bond with GLU69 amino acid, and an alkyl bond with MET4 amino

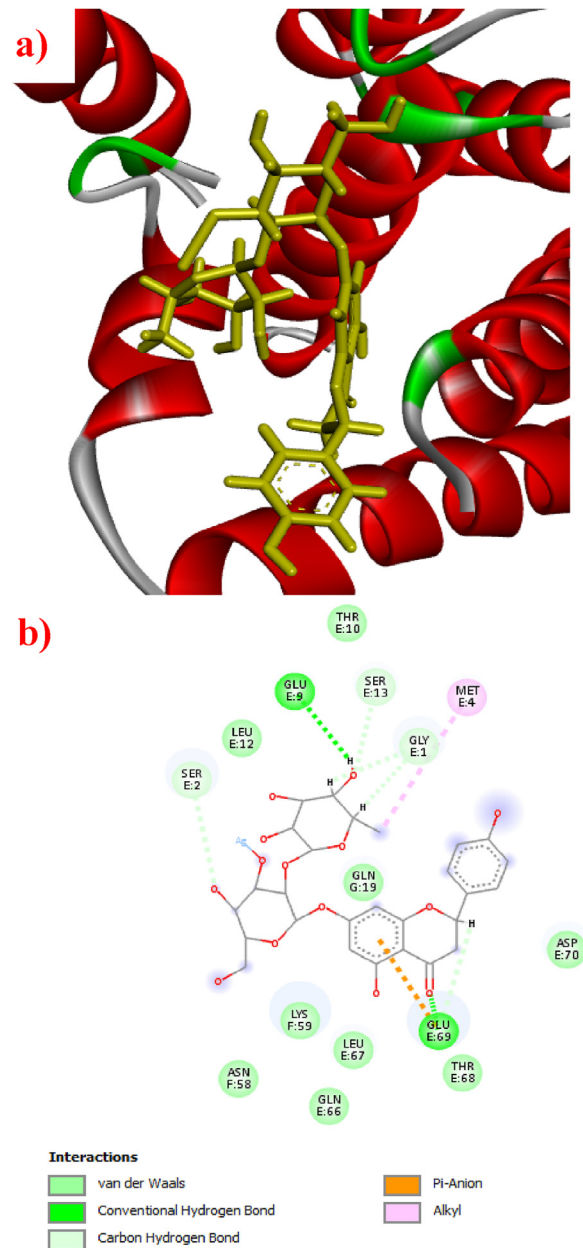


Fig. 11. The molecular docking of Amygdalin-Ag NP with 2UWJ as a target protein of *P. aeruginosa*, (a) 3D, (b) 2D.

acid in the active site of the protein. These interactions suggest a strong binding affinity between the amygdalin-Ag NP complex and the 2UWJ protein, potentially inhibiting its activity in forming the T3SS needle. This inhibition could reduce the bacterium's virulence, as it would limit the pathogen's ability to infect the host cells.

### 3.9. Screening antibacterial efficiency of Am-AgNPs

Using the agar well diffusion method, the effectiveness of Am-AgNPs synthesized by innovative green synthesis was tested in inhibiting the growth of *P. aeruginosa* isolated from wounds and burns for hospitalized patients and cultured on a Mueller-Hinton agar medium at (37 °C) for (24 h). Figs. 12 and 13 show that the largest inhibition zone occurred at a concentration of (5 mM) against *P. aeruginosa* isolated from wounds with a diameter of (20.73 mm), while it was at a diameter of (17.99 mm) against *P. aeruginosa* isolated from burns. Next, we classified the inhibition zones based on the

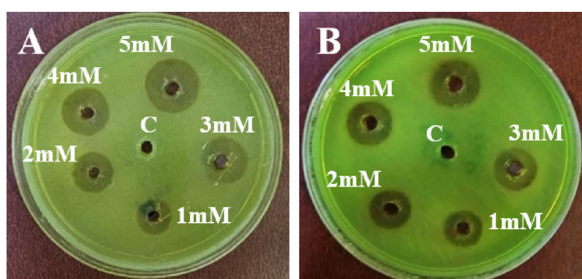


Fig. 12. Antibacterial activity of Am-AgNPs against the bacterial species under study, (a) *P. aeruginosa* isolated from wounds, (b) *P. aeruginosa* isolated from burns.

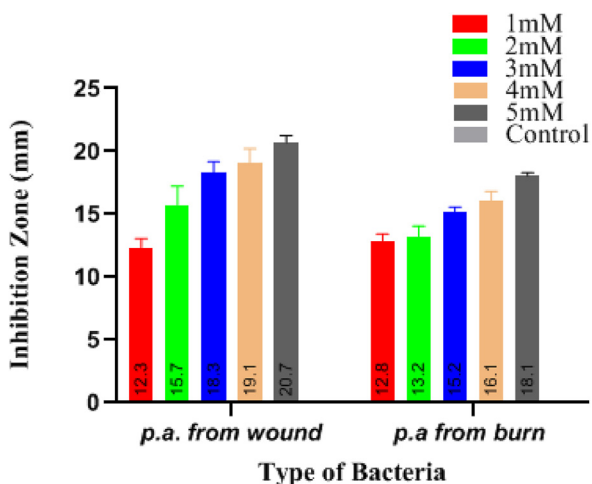


Fig. 13. Chart to compare the activity of Am-AgNPs against *P. aeruginosa* (p.a.) isolated from burns and wounds.

concentrations used against the studied bacterial species. The inhibitory effectiveness of the control is zero, so we do not notice an increase in the control column in Fig. 13.

These results are in remarkable agreement with those reported by Ref. [36], where 75 and 100 mM/disc doses of biosynthesized AgNPs showed significant activity against *P. aeruginosa* strain, recording inhibition zones of (14.68 and 17.15 mm), respectively. They revealed the antibacterial properties of these green nanoparticles, which were prepared using ginger, onion, and jujube extracts, showing inhibition zones of varying sizes ranging from (11 to 17 mm). Through the results we obtained in the research, it was observed that the nanoparticles synthesized by the innovative green method were effective against bacterial isolates. Studying the properties of the Am-AgNPs prepared in this research revealed and clarified the smaller size of the Am-AgNPs manufactured by the innovative green method. For several reasons related to mechanics and biology, the small dimensions of nanoparticles contribute to their antibacterial effectiveness. First, the distinctive feature of these particles is their large surface area relative to their size, which increases their area of influence on the bacterial cell's surface and allows them to penetrate the bacterial membrane due to their small size. When these particles enter the bacteria, they will interfere with the internal cellular processes and functions, such as bacterial metabolism, in addition to affecting the formation of the bacterial cell wall [37]. The inhibitory activity improves with a reduction in the size of the produced nanoparticles. AgNPs sustained release of  $\text{Ag}^+$  ions is responsible for their antimicrobial effect [38]. Due to the small size of AgNPs, they will stick to the outer membrane of the bacterial cell and interact with the phospholipids and proteins within it, which leads to the disruption of the osmotic system in the bacterial cell membrane and thus the explosion and death of the bacterial cells. This mechanism was demonstrated by Ref. [39]. After the AgNPs penetrate the membrane, they begin to affect the intracellular processes of the bacteria, such as inhibiting enzymes necessary for growth. The particles release silver ions that bind to the thiol groups present in bacterial proteins and enzymes, disrupting their vital functions and negatively affecting the cell's metabolism [40]. This indicates that AgNPs inhibit essential enzymes, thereby hindering the growth and reproduction of bacteria. Another mechanism is the generation of reactive oxygen species (ROS), which is one of the most important mechanisms of killing bacteria by AgNPs. The particles stimulate the formation of

reactive oxygen species such as hydrogen peroxide and hydroxyl radicals, which cause significant damage to DNA, proteins, and lipids inside the bacterial cell, disrupting its basic functions. A study by Ref. [41] showed that ROS generation is a major factor in bacterial eradication by AgNPs.

### 3.10. Screening cytotoxicity study and anticancer of Am-AgNPs

In Fig. 14, it is noted the effectiveness of Am-AgNPs synthesized by innovative green synthesis methods. The results of the current research show the inhibition rate of nanoparticles at concentrations (400, 200, 100, 50, 25, 12.5, 6.25, and 3.12  $\mu\text{g/ml}$ ) respectively towards the cancer line A375, where it was found that  $\text{IC}_{50} = 113.0$ . It is also noted that the viability decreases with increasing concentration, as it was 96.065 at a concentration of (3.12  $\mu\text{g/ml}$ ), and the viability decreased at a concentration of (400  $\mu\text{g/ml}$ ) to 39.352 within (24 h) of the experiment. The viability of the normal cell line HDFn was not substantially impacted by the concentration increase. At a concentration of (400  $\mu\text{g/ml}$ ), it was 68.48, while at a concentration of (3.12  $\mu\text{g/ml}$ ), it was 96.53533. Within (24 h) of the experiment, the  $\text{IC}_{50}$  was 151.7.

Am-AgNPs prepared using the innovative method show significantly high efficacy. The enhanced properties of the nanoparticles prepared using the innovative method, such as reduced particle size [42], are responsible for this effect. This effect is observed when the nanoparticles are studied to determine their ability to interact with cancer cells. The utilization of innovative particle preparation techniques leads to the production of stable, isomorphous particles, which enhances their capacity to penetrate cell membranes and target cancer cells with greater precision. This enhances the anti-cancer effects by stimulating the apoptosis process. AgNPs have proven effective in stopping the growth of cancer cells through several mechanisms, most

notably inducing oxidative stress within these cells. ROS cause damage to DNA, proteins, and lipids within cancer cells, disrupt vital metabolic processes and ultimately lead to cell death through the mechanism of programmed death. This mechanism has been confirmed by Ref. [43], who showed that AgNPs significantly increased levels of ROS inside cancer cells, inducing apoptosis. One of the primary targets of AgNPs is mitochondria, the main source of energy in cells. When these particles enter cells, they affect mitochondrial functions by reducing energy production (ATP) and disrupting cellular respiration. The decrease in available energy leads to a reduction in the ability of cancer cells to grow and reproduce [44]. AgNPs also affect in another way, by interacting with proteins that regulate the cell cycle in cancer cells, such as P53, as AgNPs disrupt this protein, which is necessary for regulating the cycle of cancer cells during its role in repairing their DNA, and thus will lead to genetic damage in cancer cells and then their death, according to a study by Ref. [45].

## 4. Conclusions

In this study, an innovative and novel eco-friendly approach was developed to synthesizing Am-AgNPs using a pure extract containing only amygdalin and Nd: YAG laser as the reaction activator, replacing conventional heat typically used in green synthesis. The aim of using this laser is to increase environmental sustainability to ensure that no toxic fumes and gases are produced. The synthesized nanoparticles had excellent dimensions. Molecular docking results showed strong affinity for the 4QU3, 7MQK, and 2UWJ proteins that are of great importance in the virulence and antibiotic resistance of *P. aeruginosa*. This strong affinity highlights the importance of Am-AgNPs as a promising therapeutic agent targeting MDR *P. aeruginosa*. Additionally, the results of the inhibitory activity of Am-AgNPs showed that they were very effective against MDR *P. aeruginosa* isolated from wounds and burns, and they also demonstrated a good cytotoxicity effect against the skin cancer cell line A375 compared to the normal cell line HDFn. Based on these findings, these particles were highly effective in biological applications, which opens up prospects for their use in producing new generations of drugs for treat many incurable diseases.

## Ethics information

This study was conducted in compliance with ethical principles. The study protocol, subject

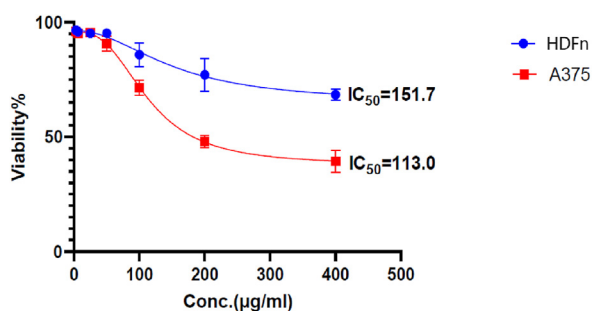


Fig. 14. Effect of Am-AgNPs on HDFn and A375 cell lines.

information, and consent form were approved by the local ethics committee according to administrative order No. THU00004 dated 10/17/2024.

## Funding

No funding has been received as the authors have provided all the necessary funding.

## Conflict of interest

The authors declare no conflicting interests.

## Acknowledgments

The authors are grateful to Tikrit University for providing scientific laboratories to conduct experiments and research.

## References

- [1] E.F. Ahmed, A.H. Rasmi, A.M.A. Darwish, G.F.M. Gad, Prevalence and resistance profile of bacteria isolated from wound infections among a group of patients in upper Egypt: a descriptive cross-sectional study, *BMC Res. Notes* 16 (2023) 1–11, <https://doi.org/10.1186/s13104-023-06379-y>.
- [2] L.J. Bessa, P. Fazii, M.D. Giulio, L. Cellini, Bacterial isolates from infected wounds and their antibiotic susceptibility pattern: some remarks about wound infection, *Int. Wound J.* 12 (2015) 47–52, <https://doi.org/10.1111/iwj.12049>.
- [3] A. Catalano, D. Iacopetta, J. Ceramella, D. Scumaci, F. Giuzio, C. Saturnino, S. Aquaro, C. Rosano, M.S. Sinicropi, Multidrug resistance (MDR): a widespread phenomenon in pharmacological therapies, *Molecules* 27 (2022) 1–18, <https://doi.org/10.3390/molecules27030616>.
- [4] J. Jain, S. Arora, J.M. Rajwade, P. Omray, S. Khandelwal, K.M. Paknikar, Silver nanoparticles in therapeutics: development of an antimicrobial gel formulation for topical use, *Mol. Pharm.* 6 (2009) 1388–1401, <https://doi.org/10.1021/mp900056g>.
- [5] F.F. Tuon, L.R. Dantas, P.H. Suss, V.S. Tasca Ribeiro, Pathogenesis of the *Pseudomonas aeruginosa* biofilm: a review, *Pathogens* 11 (2022) 1–19, <https://doi.org/10.3390/pathogens11030300>.
- [6] R. Salomoni, P. Léo, A.F. Montemor, B.G. Rinaldi, M.F.A. Rodrigues, Antibacterial effect of silver nanoparticles in *Pseudomonas aeruginosa*, *Nanotechnol. Sci. Appl.* 10 (2017) 115–121, <https://doi.org/10.2147/NSA.S133415>.
- [7] E.T. Adebayo, N.A. Hussain, Pattern of prescription drug use in Nigerian army hospitals, *Ann. Afr. Med.* 9 (2010) 152–158, <https://doi.org/10.4103/1596-3519.68366>.
- [8] A. Apisarnthanarak, J. Tunpornchai, K. Tanawitt, L.M. Mundy, Nonjudicious dispensing of antibiotics by drug stores in Pratumthani, Thailand, *Infect. Control Hosp. Epidemiol.* 29 (2008) 572–575, <https://doi.org/10.1086/587496>.
- [9] H. Deng, D. McShan, Y. Zhang, S.S. Sinha, Z. Arslan, P.C. Ray, H. Yu, Mechanistic study of the synergistic antibacterial activity of combined silver nanoparticles and common antibiotics, *Environ. Sci. Technol.* 50 (2016) 8840–8848, <https://doi.org/10.1021/acs.est.6b00998>.
- [10] R.T. Rupak Thapa, C.B. Chintan Bhagat, P.S. Pragma Shrestha, S.A. Suvash Awal, P.D. Pravin Dudhagara, Enzyme-mediated formulation of stable elliptical silver nanoparticles tested against clinical pathogens and MDR bacteria and development of antimicrobial surgical thread, *Ann. Clin. Microbiol. Antimicrob.* 16 (2017) 1–10, <https://doi.org/10.1186/s12941-017-0216-y>.
- [11] K. Gold, B. Slay, M. Knackstedt, A.K. Gaharwar, Antimicrobial activity of metal and metal-oxide based nanoparticles, *Adv. Therapeut.* 1 (2018) 1–41, <https://doi.org/10.1002/adtp.201700033>.
- [12] M. Alavi, M. Rai, Recent advances in antibacterial applications of metal nanoparticles (MNPs) and metal nanocomposites (MNCs) against multidrug-resistant (MDR) bacteria, *Expert Rev. Anti-infect. Ther.* 17 (2019) 19–428, <https://doi.org/10.1080/14787210.2019.1614914>.
- [13] M. Ider, K. Abderrafi, A. Eddahbi, S. Ouaskit, A. Kassiba, Silver metallic nanoparticles with surface plasmon resonance: synthesis and characterizations, *J. Cluster Sci.* 28 (2017) 1051–1069, <https://doi.org/10.1007/s10876-016-1080-1>.
- [14] C.N. Miller, N. Newall, S.E. Kapp, G. Lewin, L. Karimi, K. Carville, T. Gliddon, N.M. Santamaria, A randomized-controlled trial comparing cadexomer iodine and nanocrystalline silver on the healing of leg ulcers, *Wound Repair Regen.* 18 (2010) 359–367, <https://doi.org/10.1111/j.1524-475X.2010.00603.x>.
- [15] T. Bruna, F. Maldonado-Bravo, P. Jara, N. Caro, Silver nanoparticles and their antibacterial applications, *Int. J. Mol. Sci.* 22 (2021) 1–21, <https://doi.org/10.3390/ijms22137202>.
- [16] Y. Ren, Y. Zhang, X. Li, Application of AgNPs in biomedicine: an overview and current trends, *Nanotechnol. Rev.* 13 (2024) 1–17, <https://doi.org/10.1515/ntrev-2024-0030>.
- [17] N.S. Swidan, Y.A. Hashem, W.F. Elkhatib, M.A. Yassien, Antibiofilm activity of green synthesized silver nanoparticles against biofilm associated enterococcal urinary pathogens, *Sci. Rep.* 12 (2022) 1–13, <https://doi.org/10.1038/s41598-022-07831-y>.
- [18] Z. Song, X. Xu, Advanced research on anti-tumor effects of amygdalin, *J. Cancer Res. Therapeut.* 10 (2014) 1–5, <https://doi.org/10.4103/0973-1482.139743>.
- [19] X.Y. He, L.J. Wu, W.X. Wang, P.J. Xie, Y.H. Chen, F. Wang, Amygdalin-A pharmacological and toxicological review, *J. Ethnopharmacol.* 254 (2020) 1–13, <https://doi.org/10.1016/j.jep.2020.112717>.
- [20] H.K. Du, F.C. Song, X. Zhou, H. Li, J.P. Zhang, Effect of amygdalin on serum proteinic biomarker in pulmonary fibrosis of bleomycin-induced rat, *Chin. J. Ind. Hyg. Occup. Dis.* 28 (2010) 260–263, <https://europepmc.org/article/med/20465950>.
- [21] T.Y.K. Chan, A probable case of amygdalin-induced peripheral neuropathy in a vegetarian with vitamin B12 deficiency, *Ther. Drug Monit.* 28 (2006) 140–141, <https://doi.org/10.1097/01.ftd.0000179419.40584.15>.
- [22] S.N. Rashid, K.A. Aadim, A.S. Jasim, A.M. Hamad, Synthesized zinc nanoparticles via pulsed laser ablation: characterization and antibacterial activity, *Karbala Intern. J. Modern Sci.* 8 (2022) 462–476, <https://doi.org/10.33640/2405-609X.3240>.
- [23] Q. Dong, J. Hu, Z. Guo, J. Lian, J. Chen, B. Chen, Surface morphology study on chromium oxide growth on Cr films by Nd-YAG laser oxidation process, *Appl. Surf. Sci.* 202 (2002) 114–119, [https://doi.org/10.1016/S0169-4332\(02\)00941-8](https://doi.org/10.1016/S0169-4332(02)00941-8).
- [24] F.T.L. Muniz, M.A.R. Miranda, C. Morilla dos Santos, J.M. Sasaki, The Scherrer equation and the dynamical theory of X-ray diffraction, *Acta Crystallogr. A: Foundation Adv.* 72 (2016) 385–390, <https://doi.org/10.1107/S205327331600365X>.
- [25] M.S. Valdés-Tresanco, M.E. Valdés-Tresanco, P.A. Valiente, E. Moreno, AMDock: a versatile graphical tool for assisting molecular docking with Autodock Vina and Autodock4, *Biol. Direct* 15 (2020) 1–12, <https://doi.org/10.1186/s13062-020-0267-2>.
- [26] M. Vanaja, G. Gnanajobitha, K. Paulkumar, S. Rajeshkumar, C. Malarkodi, G. Annadurai, Phytosynthesis of silver nanoparticles by *Cissus quadrangularis*: influence of physico-chemical factors, *J. Nanostruct. in Chem.* 3 (2013) 1–8, <https://doi.org/10.1186/2193-8865-3-17>.
- [27] M. Cakić, S. Glišić, G. Nikolić, G.M. Nikolić, K. Cakić, M. Cvetinović, Synthesis, characterization and antimicrobial activity of dextran sulphate stabilized silver nanoparticles, *J. Mol. Struct.* 1110 (2016) 156–161, <https://doi.org/10.1016/j.jmolstruc.2016.01.040>.

- [28] S. Hamed, S.M. Ghaseminezhad, S.A. Shojaosadati, S. Shokrollahzadeh, Comparative study on silver nanoparticles properties produced by green methods, Iran. J. Biotechnol. 3 (2012) 1–9. [https://www.sid.ir/en/vevssid/j\\_pdf/92820120306.pdf](https://www.sid.ir/en/vevssid/j_pdf/92820120306.pdf).
- [29] D.A. Aina, O. Owolo, A. Lateef, F.O. Aina, A.S. Hakeem, M. Adeoye-Isijola, V. Okon, T.B. Asafa, J.A. Elegbede, O.D. Olukanni, Biomedical applications of Chasmanthera dependens stem extract mediated silver nanoparticles as antimicrobial, antioxidant, anticoagulant, thrombolytic, and larvicidal agents, Karbala Intern. J. Modern Sci. 5 (2019) 71–80, <https://doi.org/10.33640/2405-609X.1018>.
- [30] B. Mosayyebi, M. Imani, L. Mohammadi, A. Akbarzadeh, N. Zarghami, E. Alizadeh, M. Rahmati, Comparison between  $\beta$ -cyclodextrin-amygdalin nanoparticle and amygdalin effects on migration and apoptosis of MCF-7 breast cancer cell line, J. Cluster Sci. 33 (2022) 935–947, <https://doi.org/10.1007/s10876-021-02019-2>.
- [31] C. Sekar, R. Parimaladevi, Effect of silver nitrate ( $\text{AgNO}_3$ ) on the growth, optical, spectral, thermal and mechanical properties of  $\gamma$ -glycine single crystal, J. Optoelectro. Biomed. Mater. 1 (2009) 215–225. <https://chalcogen.ro/2Sekar.pdf>.
- [32] S. Biswas, A.F. Mulaba-Bafubandi, Optimization of process variables for the biosynthesis of silver nanoparticles by *Aspergillus wentii* using statistical experimental design, Adv. Nat. Sci. Nanosci. Nanotechnol. 7 (2016) 1–11, <https://doi.org/10.1088/2043-6262/7/4/045005>.
- [33] M. Zieliński, J. Blanchet, S. Hailemariam, A.M. Berghuis, Structural elucidation of substrate-bound aminoglycoside acetyltransferase (3)-IIIa, PLoS One 17 (2022) 1–14, <https://doi.org/10.1371/journal.pone.0269684>.
- [34] N.K. Stewart, C.A. Smith, H. Frase, D.J. Black, S.B. Vakulenko, Kinetic and structural requirements for carbapenemase activity in GES-type  $\beta$ -lactamases, Biochemistry 54 (2015) 588–597, <https://doi.org/10.1021/bi501052t>.
- [35] M. Quinaud, S. Plé, V. Job, C. Contreras-Martel, J.P. Simorre, I. Attree, A. Dessen, Structure of the heterotrimeric complex that regulates type III secretion needle formation, Proc. Natl. Acad. Sci. USA 104 (2007) 7803–7808, <https://doi.org/10.1073/pnas.061009810>.
- [36] M.A. Khalil, G.M. El Maghraby, F.I. Sonbol, N.G. Allam, P.S. Ateya, S.S. Ali, Enhanced efficacy of some antibiotics in presence of silver nanoparticles against multidrug resistant *Pseudomonas aeruginosa* recovered from burn wound infections, Front. Microbiol. 12 (2021) 1–20, <https://doi.org/10.3389/fmicb.2021.648560>.
- [37] K.R. Raghupathi, R.T. Koodali, A.C. Manna, Size-dependent bacterial growth inhibition and mechanism of antibacterial activity of zinc oxide nanoparticles, Langmuir 27 (2011) 4020–4028, <https://doi.org/10.1021/la104825u>.
- [38] S. Qamer, M.H. Romli, F. Che-Hamzah, N. Misni, N.M.S. Joseph, N.A. Al-Haj, S. Amin-Nordin, Systematic review on biosynthesis of silver nanoparticles and antibacterial activities: application and theoretical perspectives, Molecules 26 (2021) 1–21, <https://doi.org/10.3390/molecules26165057>.
- [39] W.R. Li, X.B. Xie, Q.S. Shi, H.Y. Zeng, Y.S. Ou-Yang, Y.B. Chen, Antibacterial activity and mechanism of silver nanoparticles on *Escherichia coli*, Appl. Microbiol. Biotechnol. 85 (2010) 1115–1122, <https://doi.org/10.1007/s00253-009-2159-5>.
- [40] Q.L. Feng, J. Wu, G.Q. Chen, F.Z. Cui, T.N. Kim, J.O. Kim, A mechanistic study of the antibacterial effect of silver ions on *Escherichia coli* and *Staphylococcus aureus*, J. Biomed. Mater. Res. 52 (2000) 662–668, [https://doi.org/10.1002/1097-4636\(20001215\)52:4<662::AID-JBM10>3.0.CO;2-3](https://doi.org/10.1002/1097-4636(20001215)52:4<662::AID-JBM10>3.0.CO;2-3).
- [41] O. Choi, K.K. Deng, N.J. Kim, L. Ross Jr., R.Y. Surampalli, Z. Hu, The inhibitory effects of silver nanoparticles, silver ions, and silver chloride colloids on microbial growth, Water Res. 42 (2008) 3066–3074, <https://doi.org/10.1016/j.watres.2008.02.021>.
- [42] R.K. Jain, T. Stylianopoulos, Delivering nanomedicine to solid tumors, Nat. Rev. Clin. Oncol. 7 (2010) 653–664, <https://doi.org/10.1038/nrclinonc.2010.139>.
- [43] M.M. Rohde, C.M. Snyder, J. Sloop, S.R. Solst, G.L. Donati, D.R. Spitz, C.M. Furdul, R. Singh, The mechanism of cell death induced by silver nanoparticles is distinct from silver cations, Part. Fibre Toxicol. 18 (2021) 1–24, <https://doi.org/10.1186/s12989-021-00430-1>.
- [44] F. Wang, Z. Chen, Y. Wang, C. Ma, L. Bi, M. Song, G. Jiang, Silver nanoparticles induce apoptosis in HepG2 cells through particle-specific effects on mitochondria, Environ. Sci. Technol. 56 (2022) 5706–5713, <https://doi.org/10.1021/acs.est.1c08246>.
- [45] K. Kalishwaralal, E. Banumathi, S.R.K. Pandian, V. Deepak, J. Muniyandi, S.H. Eom, S. Gurunathan, Silver nanoparticles inhibit VEGF induced cell proliferation and migration in bovine retinal endothelial cells, Colloids Surf. B Biointerfaces 73 (2009) 51–57, <https://doi.org/10.1016/j.colsurfb.2009.04.025>.